Radar Backscattering of Lake Ice During Freezing and Thawing Stages Estimated by Ground-Based Scatterometer Experiment and Inversion From Genetic Algorithm

Hyangsun Han, *Student Member, IEEE*, and Hoonyol Lee, *Senior Member, IEEE*

***Abstract*—Lake ice under phase transition shows large variation on radar backscattering due to the changes of dielectric constant and roughness of ice surface and thus the transmissivity of microwave into ice body. To study the effects of freezing/thawing of ice on radar backscattering in a short time, we spread water over lake ice and continuously measured radar backscattering by using a ground-based microwave scatterometer system operated in C-band HH polarization. By establishing scattering models and applying inversion from genetic algorithm, radar returns were separated into ice-surface, volume, and ice-bottom scatterings, and the changes in dielectric constant and roughness parameters of ice surface were estimated as well. Immediately after spreading water on ice surface, ice-surface scattering was strongest due to high dielectric constant of surface water while volume and ice-bottom scatterings were very weak due to low microwave transmissivity into ice body. As surface water was being frozen, ice-surface scattering became weak with decreasing dielectric constant while volume and ice-bottom scattering increased due to higher transmissivity into ice body. In a transition stage, when surface water was almost frozen, all three scatterings increased simultaneously. Crystallization of ice produced rougher surface overcoming the decrease in dielectric constant, resulting in the increase of ice-surface scattering, while volume and ice-bottom scattering was continuously increased due to increasing transmissivity. At the end of the experiment, air temperature rose above freezing point, and ice surface thawed again so that ice-surface scattering increased while volume and ice-bottom scattering were decreased.**

***Index Terms*—Backscattering, freezing, genetic algorithm (GA), lake ice, scatterometer, thawing.**

I. Introduction

CHANGE of lake ice state (phase) is a principal factor for the study of regional climate as it is significantly affected by the climatic elements such as air and water temperature, wind speed, humidity, the duration of sunshine, and heat budget of the lake [1]–[5]. The freezing and thawing dates of lake provide the information of variability pattern of local climate [6], [7]. Moreover, the freeze-up and break-up of lake ice have a considerable impact on aquatic ecosystem [8], [9]. When the climatic elements change over the lake ice, the state of lake ice varies in company with physical properties such as dielectric constant, surface roughness, ice thickness, size, and shape of air bubbles [10]. Especially, the dielectric constant and roughness of ice surface experience considerable changes during the phase transition of ice because they are highly sensitive to the variation in climatic elements. Therefore, it is necessary to investigate physical properties of lake ice with regard to its state and its changes.

Radar backscattering can be an indicator representing various physical properties of lake ice at once [11]. Surface scattering of lake ice is affected by roughness and dielectric constant of ice surface. Volume scattering is caused by air bubbles captured inside ice, while ice-bottom scattering is controlled by roughness and dielectric constant of the ice/water interface. Volume and ice-bottom scattering increases in winter season as microwave transmissivity into ice is high due to low dielectric constant of ice surface in freezing stage [12]–[14]. When the lake ice freezes to the lake bed in winter season, the ice-bottom scattering becomes weak because the contrast of dielectric constant on the ice/bed interface is very small [15], [16]. In thawing season, the ice-surface scattering is strong, while volume and ice-bottom scattering become weak, which is due to the high dielectric constant of the ice surface that leads to decreasing in the penetration depth of microwave into the ice [12], [13].

As stated above, the radar backscattering is seriously influenced by the physical properties of lake ice which are changed by phase transition. The rapid phase transition of lake ice surface can occur in a short time when the difference of air temperature is huge and wind speed is strong for a day [1]. Then, the physical properties of ice surface are dramatically changed by the rapid phase transition, which leads to variation in the radar backscattering from ice. In such cases, active microwave remote sensing system with higher temporal resolution is necessary to repeatedly measure the radar backscattering from lake ice in a brief time.

Satellite synthetic aperture radar (SAR) systems provide high temporal-resolution images that include the backscattering

Manuscript received February 14, 2012; revised May 21, 2012 and June 27, 2012; accepted July 15, 2012. Date of publication September 28, 2012; date of current version April 18, 2013. This work was supported by the Basic Science Research Program through the National Research Foundation of Korea (NRF) funded by the Ministry of Education, Science and Technology (No. 2010-0009465) and was also supported by Korea Polar Research Institute Project (PE12050).

The authors are with the Department of Geophysics, Kangwon National University, Chuncheon 200-701, Korea (e-mail: hoonyol@kangwon.ac.kr).

Color versions of one or more of the figures in this paper are available online at http://ieeexplore.ieee.org.

Digital Object Identifier 10.1109/TGRS.2012.2214393

by various interactions between microwave and lake ice [17], [18]. The origin of backscattering observed by SAR should be classified into the various scatterings for more accurate estimation of ice state and physical properties of the ice because the radar backscattering from SAR includes ice-surface, volume, and ice-bottom scattering [19]. However, it is very difficult to identify the backscattering observed by SAR as the various scatterings. Moreover, the temporal resolution of SAR is unqualified to estimate the physical properties of lake ice when the phase of ice surface varies quickly.

Ground-based microwave scatterometer is widely used to measure the scattering properties of various targets and to validate the satellite SAR data because it has the advantages of convenient operation of polarization, wavelength, and incidence angle [20]. As the spatial and temporal resolutions of the ground-based microwave scatterometer are better than those of satellite SAR, it can be the best active microwave remote sensing system to estimate the scattering properties of lake ice experiencing rapid phase transition. Many researchers analyzed the microwave scattering properties of ice by using the ground-based microwave scatterometer [20]–[25]. Onstott [22] reported the ground-based microwave scatterometer experiments for sea ice from 1970s to 1980s which showed that the backscattering from sea ice varied as a function of frequency, incidence angle, polarization, and season. Geldsetzer *et al.* [23] performed C-band ground-based microwave scatterometer experiment for various types of sea ice and revealed that the backscattering from snow-covered first-year ice (FYI), multi-year ice (MYI) and melt pond on FYI decreased with increasing in incidence angle, showing that the co-polarized backscattering was higher than the cross-polarized backscattering in all incidence angles. Isleifson *et al.* [24] analyzed the backscattering properties from MYI by using C-band ground-based microwave scatterometer and concluded that the backscattering from MYI was higher at VV-polarization than at HH-polarization. Other researches using the ground-based microwave scatterometer also reported the radar backscattering properties which vary as the wavelengths, polarizations, and incidence angles of microwave. However, the variation of scattering properties of lake ice by change of the physical properties due to phase transition was not explained yet.

In several studies, radar backscattering modeling was performed to more accurately analyze the scattering properties of ice [11], [20], [26, 27, 29]. The researches explained the influence of the physical properties of ice on backscattering and the contribution of ice-surface, volume and ice-bottom scattering to the total backscattering measured by SAR or scatterometer. However, the changes in scattering properties by the phase transition of ice were still not described yet. Furthermore, most researches used the general physical properties of ice to simulate the radar backscattering regardless of the phase state of the ice. The physical properties corresponding to phase state of the ice are required to perform accurate radar backscattering modeling. The physical properties of the ice can be investigated by *in situ* measurement, but it is very difficult when the phase transition of ice occurs in a short time due to rapid changes in the physical properties.

Fig. 1. Photograph of ice surface at the experiment site. The ice surface was clear of snow. A trihedral corner reflector on ice surface was used to calibrate the system.

In this paper, we analyze the microwave scattering properties of lake ice during phase transition of ice surface in a brief time by using a ground-based microwave scatterometer and inversion modeling. The study site and the results of the scatterometer experiment on lake ice were presented in Section II. Forward modeling and the results of inversion by genetic algorithm (GA) was described in Section III to estimate the physical properties of the ice in the phase transition and to identify radar returns from ice-surface, volume, and ice-bottom scattering. Section IV concludes this paper.

II. Scatterometer Experiment on Lake Ice

A. Experiment Setup and Ground Reference Data

A ground-based microwave scatterometer experiment on lake ice was performed on February 2, 2006 at Chuncheon Lake located in the northeastern part of South Korea. The day was sunny with little cloud when the experiment was performed from 10:30 A.M. to 12:10 P.M. Air temperature increased with time from -3 °C to 1 °C during the experiment. The ice surface was clear of snow (Fig. 1). The average ice thickness measured through holes was 40 cm. The spherical air bubbles were sparsely distributed in the ice body. Roughness parameters of ice surface (air/ice interface) were measured by using a profiler before the scatterometer experiment: the *rms* height was 0.9 cm, and the correlation length was 3.0 cm. The average diameter of the air bubbles inside the ice was 1.4 cm, and the volume fraction of the air bubbles was approximately 1%. Several ice cubes sized approximately 50 cm $\times$ 50 cm (width $\times$ length) were cut near the experiment site for fishing activities by local residents. The roughness of ice/water interface was measured on the ice cubes. The *rms* height and correlation length of ice/water interface were 2.1 cm and 10.8 cm, respectively.

The scatterometer is composed of a C-band (5.3 GHz) square horn antenna, a vector network analyzer (VNA), notebook computer, and a 2 m stand (Fig. 2). The bandwidth of antenna was set to 600 MHz, so that the range and time resolution were 25 cm and 1.67 ns, respectively (Table I). The VNA (Model 8753ES of Agilent Technology Inc.) generates signal in a stepped-frequency sweeping and measures the returned S-parameter in time domain after inverse Fourier transformation. The notebook computer controls all other instruments and collects the data. The antenna height was 2 m, and the incidence

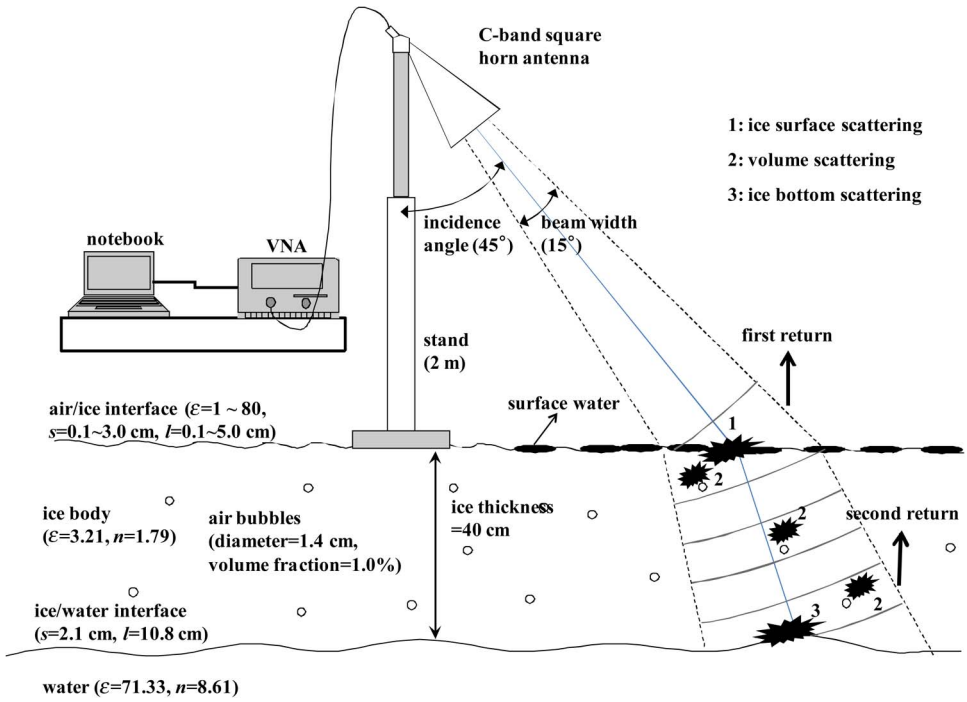

Fig. 2. Conceptual model of the ground-based scatterometer experiment on lake ice. The scatterometer measures the backscattering signals from air/ice and ice/water interface as well as volume scattering. The ranges of physical properties of the air/ice interface are the boundary condition during the GA inversion.

TABLE I
SPECIFICATION OF THE GROUND-BASED MICROWAVE SCATTEROMETER

Specification	Value
vector network analyzer	Agilent 8753ES
antenna type	square horn antenna
center frequency	5.3 GHz (C-band)
bandwidth	600 MHz
polarization	HH
beam width	15°
antenna gain	21.76 dBi
noise floor	-50 dB
range resolution	25 cm
incidence angle	45°
antenna altitude	2 m

angle was 45°. Using a trihedral corner reflector, the gain of the antenna at beam center (G) was precisely measured to be 21.76 dBi. The temperature of the frozen ice surface was measured to be 0 °C by a thermometer just before the measurement. Based on the empirical formulas proposed by Ray [30] and Sadiku [31], the dielectric constant of the ice surface at 0 °C is given as 3.174 at 5.3 GHz, which is the center frequency of the scatterometer system.

We spread water over the ice surface to simulate the freezing/thawing stages in a brief time, and then repeatedly measured the radar returns from the ice in every 10 min from

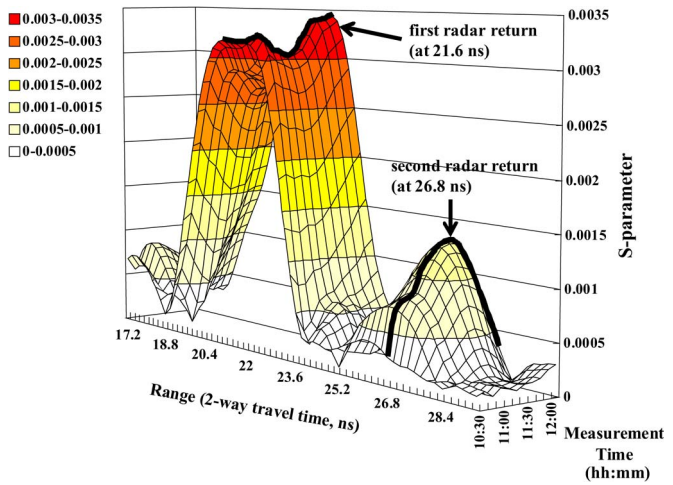

Fig. 3. S-parameter measured by the ground-based microwave scatterometer. The first and second radar returns (S_1 and S_2) were measured at 21.6 ns (ice surface) and 26.8 ns (ice/water interface), respectively.

10:30 A.M. to 12:10 P.M. Air temperature was −3 °C at 10:30 A.M. when the experiment began and rose monotonically above freezing point at 11:50 A.M. and up to 1 °C by the end of the experiment at 12:10 P.M. The surface water spread over the ice began to freeze and turned into ice within an hour, but the surface melted again due to solar radiation and the air temperature above freezing point. Therefore, the ice surface has undergone the following three stages: freezing stage, frozen stage, and thawing stage during the experiment.

B. Results of Scatterometer Data

Fig. 3 shows the S-parameter from the lake ice measured by the scatterometer as a function of two-way travel time in

nano-seconds and the observation time (hour : minute). Two strong radar returns were observed in each measurement: The first radar return from air/ice boundary (S_1) appeared at 21.6 ns, while the second radar return (S_2) from ice/water boundary was measured at 26.8 ns. By using the difference of two-way travel time of the first and the second returns $(\Delta T = 5.2$ ns), the refraction angle of microwave in ice body (θ_t) was calculated as 23.24° by the following equation:

$$\theta_t = \frac{1}{2}\sin^{-1}\left(\frac{4d\sin\theta_i}{c\Delta T}\right) \tag{1}$$

where d is the ice thickness (40 cm), c is the speed of light and θ_i is the incidence angle (45°). Then, the refractive index $(n = 1.79)$ and dielectric constant $(\varepsilon = 3.21)$ of ice body can be deduced by the following equation:

$$n = \sqrt{\mu_r \varepsilon} = \sin\theta_i / \sin\theta_t \tag{2}$$

assuming that the relative permeability μ_r is equal to 1. The dielectric constant of ice body should be constant during the experiment while that of ice surface was changed according to the freezing/thawing stages.

Generally, S_1 was stronger than S_2. As time goes by, S_1 became weak, and then it became stronger again due to the freezing/thawing sequence. However, S_2 increased continuously, but it weakened just before the last measurement. The asymmetry section in which the first and second returns increased at same time was observed from 11:20 A.M. to 11:50 A.M. This asymmetry was not easily interpretable from the surface and bottom scattering alone, and the role of volume scattering may have affected this result. It will be discussed in the next section.

III. Estimation of Ice Properties and Scattering by Genetic Algorithm

From the *in situ* measurements, we could determine the properties of frozen ice surface and ice bottom in terms of dielectric constant, *rms* height, and correlation length. However, the properties of ice surface during freezing/thawing stages vary as a function of time and are very difficult to measure nondestructively.

In addition to the surface scatterings from the air/ice and ice/water boundaries, the contribution from the volume scattering smeared into both the first and second returns. The scatterometer data cannot differentiate between ice-surface scatterings and volume scattering. Therefore, we set up a forward modeling of ice-surface scattering, volume scattering, and ice-bottom scattering of lake ice as a function of the various ice properties. Then, we performed inversion by GA to find out unknown properties of ice surface (dielectric constant, *rms* height, and correlation length) during freezing/thawing stages and to identify the scattering properties of the lake ice.

A. Forward Modeling

The radar returns from lake ice measured by ground-based microwave scatterometer can be modeled into ice-surface scattering from the air/ice interface, the volume scattering from ice body, and the ice-bottom scattering from the ice/water interface. Generally, ice-surface scattering and ice-bottom scattering contributes more to the total radar backscattering from lake ice than volume scattering due to large roughness of air/ice interface and high dielectric constant of ice/water interface [11].

Based on the lake ice characteristics at the scatterometer experiment site and the specification of our scatterometer system, we made a scatterometer measurement model as shown in Fig. 2. The first radar return includes the ice-surface scattering and volume scattering. The second radar return reflects the ice-bottom scattering as well as the volume scattering. The first and second radar returns (S_1 and S_2) measured by the scatterometer can be expressed as

$$S_1^2 = \frac{\lambda^2}{(4\pi)^3}\left[\frac{G^2 A}{R_1^4}\left(\sigma^0_{surface} + \sigma^0_{volume}\right)\right] \tag{3}$$

$$S_2^2 = \frac{\lambda^2}{(4\pi)^3}\left[\frac{G^2 A}{R_2^4}\left(\sigma^0_{volume} + \sigma^0_{bottom}\right)\right] \tag{4}$$

where R_1 and R_2 are the range from the antenna to the air/ice and to the ice/water interfaces, respectively. $\sigma^0_{surface}$ is the ice-surface scattering from air/ice interface, σ^0_{volume} the volume scattering from ice body, and σ^0_{bottom} the ice-bottom scattering from ice/water interface. A is the cross section of the radar beam. Ice-surface, volume, and ice-bottom scatterings were calculated by the following theoretical models.

The ice-surface scattering coefficient $(\sigma^0_{surface})$ from the air/ice interface can be modeled by IEM is given as [32]

$$\sigma^0_{surface\_pp} = \frac{k^2}{2}\exp\left(-2k_z^2 s^2\right)\sum_{n=1}^{\infty}\left|I^n_{pp}\right|^2\frac{W^{(n)}(-2k_x, 0)}{n!} \tag{5}$$

where pp is the polarization, k is the wavenumber, s is the *rms* height, k_x and k_z are the wavenumber components in the x and z direction, respectively. $W^{(n)}$ is the 2-D Fourier transform of the nth power of the surface autocorrelation function. Here, I^n_{pp} is given as

$$I^n_{pp} = (2k_z s)^n f_{pp}\exp\left(-k_z^2 s^2\right) + \frac{(k_z s)^n\left[F_{pp}(-k_x, 0) + F_{pp}(k_x, 0)\right]}{2} \tag{6}$$

where f_{pp} and F_{pp} are the Kirchhoff field coefficient and complementary field coefficient, respectively.

The volume scattering coefficient (σ^0_{volume}) is given as [32]

$$\sigma^0_{volume\_pp} = \frac{1}{2}(k_s/k_e)T_{1t}T_{t1}\cos\theta_i \times \left[1 - \exp(-2k_e d)/\cos\theta_t\right]P_{pp}(\cos\theta_t, -\cos\theta_t : \pi) \tag{7}$$

where k_s is the volume scattering coefficient, k_e is the extinction coefficient, T_{1t} and T_{t1} are the Fresnel power transmission coefficients when the microwave is transmitted into the ice from the antenna and the reverse case, respectively. The P_{pp} term

is the phase function of the Rayleigh scattering. Those terms depend on the diameter and volume fraction of air bubbles, ice thickness, and the dielectric constant of ice surface affecting the microwave transmissivity [11], [20], [33]. When ice body contains many tubular air bubbles, the volume scattering makes a significant contribution to the total radar backscattering [11], [34]. However, the influence of volume scattering by the spherical air bubbles on the total radar backscattering is much smaller than that by the tubular air bubbles. Therefore, spherical air bubbles are often neglected in the analysis of the microwave scattering properties of ice when size and volume fraction of the spherical air bubbles is very small [11]. As the sparsely distributed spherical air bubbles in lake ice were observed at the scatterometer experiment site, we calculated the Rayleigh scattering by the spherical air bubbles. In this paper, we perform the radar backscattering modeling of two cases that the volume scattering is neglected or included in the first and second radar returns measured by the scatterometer.

The ice-bottom scattering coefficient (σ^0_{bottom}) is calculated as [32]

$$\sigma^0_{bottom\_pp} = \cos\theta_i T_{1t} T_{t1} \times \exp(-2k_e d/\cos\theta_t)\sigma^0_{surface\_pp}(\theta_t)/\cos\theta_t \quad (8)$$

where $\sigma^0_{surface\_pp}(\theta_t)$ is the surface scattering coefficient of the ice/water interface that is calculated by replacing the incidence angle with the refracting angle of microwave in (5). The ice-bottom scattering is caused by the roughness and dielectric constant of ice/water interface. The scattering comes back to the antenna after it is attenuated in part by the air bubbles and ice thickness.

B. Inversion by GA

Microwave scattering properties of lake ice depend on various physical properties such as dielectric constant and roughness of air/ice and ice/water interface, the diameter and volume fraction of the air bubbles, and ice thickness. Before the scatterometer experiment, we surveyed the roughness of air/ice and ice/water interfaces, ice thickness, the diameter, and volume fractions of air bubbles, and estimated the dielectric constant of ice body, air/ice, and ice/water interface. However, the roughness and dielectric constant of ice surface would be changed by the freezing/thawing stages of ice surface during the scatterometer experiment. To calculate the theoretical radar backscattering from lake ice, it is necessary to estimate the changes in surface roughness and dielectric constant of ice surface. The unknown physical properties can be estimated by inversion modeling. We perform the inversion modeling by using GA to estimate the change of roughness and dielectric constant of ice surface that varied with the phase transition of ice surface from freezing to thawing condition.

GA is a global optimization technique to obtain the solution of searching problems by realizing the natural phenomena of which the fundamental notion is the Darwin's theory of survival of the fittest [35]. We considered the ice model as shown in Fig. 2 to perform the GA. The roughness and the dielectric constant of ice surface vary as the phase transition of ice surface during scatterometer experiment. Other physical properties of lake ice are not affected by the phase change of ice surface. The boundary conditions of each physical property for inversion modeling are shown in Fig. 2. The objective function of GA was defined as root mean square error (RMSE) between the radar returns measured by scatterometer and calculated by radar backscattering modeling. Initial population iteratively evolves into next generation through selection, crossover, and mutation processes until a chromosome satisfies a certain criterion on the fitness function.

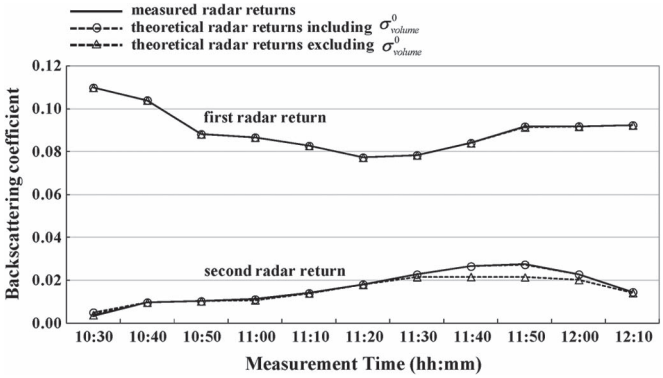

Fig. 4. Backscattering coefficients of first and second radar returns measured by the ground-based microwave scatterometer (black lines) and calculated by the GA inversion (dotted lines).

Fig. 4 shows the variation of the measured (black lines) and theoretical (dotted lines) backscattering coefficients of the first and second radar returns. The theoretical values calculated based on $\sigma^0_{surface}$ and σ^0_{bottom} are represented as triangles, while those including σ^0_{volume} are depicted in circles. When σ^0_{volume} is neglected in each radar return, the normalized RMSE (NRMSE) between the measured and calculated radar return was 1.67%. In this case, the first return was well matched, but the second return showed deviation especially when the first and second returns increase simultaneously. The theoretical radar returns that include the volume scattering were well fitted to the radar returns measured by the scatterometer showing NRMSE of 0.29%. By the result of inversion, we could confirm that each radar return measured by the scatterometer includes σ^0_{volume} as well. In the following two sections, we discuss the ice properties and the corresponding ice-surface, volume, and ice-bottom scatterings induced from GA inversion.

C. GA Results—Ice Properties

Fig. 5(a) shows the variation of dielectric constant of lake ice surface estimated by the GA in black dots. Air temperature measured in every 10 min during the scatterometer experiment is also shown in white dots. At the beginning of the experiment, the dielectric constant of ice surface was similar to that of water and then decreased continuously because surface water was being frozen into the ice. The dielectric constant of lake ice surface was smallest $(\varepsilon_r = 3.73)$ at 11:50 A.M. when the surface water was frozen completely. After that, the ice surface began to melt when air temperature rose above 0 °C resulting in the increase of dielectric constant up to 14.81.

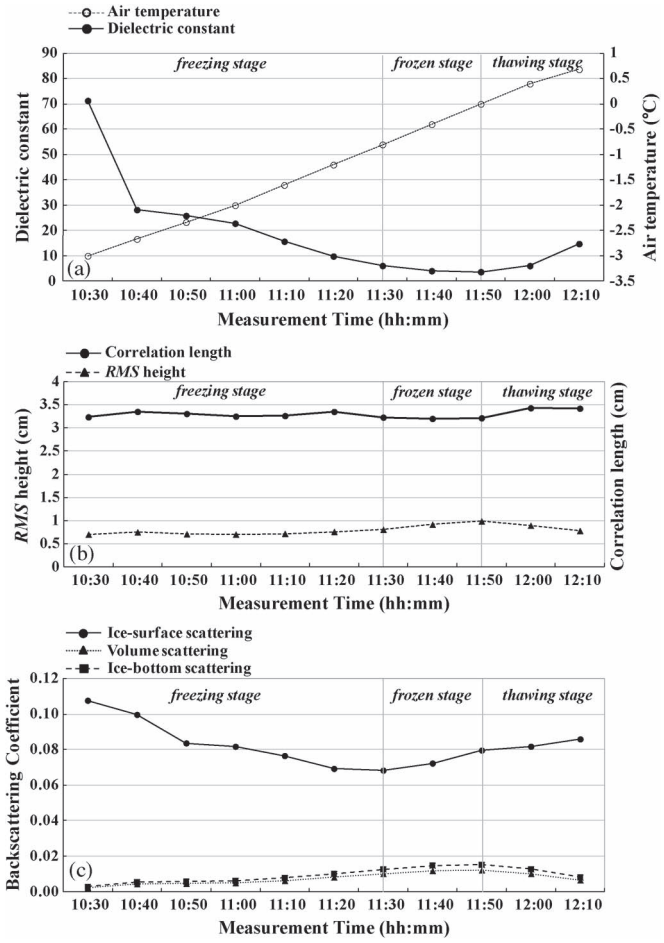

Fig. 5. Physical properties and scattering mechanisms of lake ice induced by GA: (a) dielectric constant of ice surface and air temperature, (b) the *rms* height and correlation length of ice surface, and (c) variation of ice-surface scattering, volume scattering, and ice-bottom scattering during the phase transition of ice surface.

Fig. 5(b) shows *rms* height (triangles) and the correlation length (dots) of ice surface estimated by GA. The *rms* height slowly increased in the freezing stage and increased rather rapidly from 11:30 A.M. when the surface water was almost frozen until 11:50 A.M. This implies that the phase transition of the ice surface influenced not only the dielectric constant but also the surface structure. When the dielectric constant decreases, the surface water in liquid state underwent phase transition to ice, and ice crystals were formed at the surface. The rapid increase of the *rms* height in the frozen stage suggests that ice crystallization has completed in this time window. The *rms* height and the correlation length in the frozen stage were 0.98 cm and 3.2 cm at 11:50 A.M. which were similar to those measured in frozen ice before the scatterometer experiment. From 11:50 A.M., the *rms* height decreases along with the increase of dielectric constant when the air temperature rose above freezing and the surface ice began to melt. The change in correlation length is rather random having value ranges from 3.2 to 3.4 which is difficult to interpret. The contribution of correlation length to ice-surface scattering is rather small when compared with *rms* height [36].

In summary we can divide the changes of ice surface into the freezing stage, frozen stage, and thawing stage. In the freezing stage, the dielectric constant of the ice surface decreased, and the *rms* height increased slowly due to the gradual change of state from liquid water to solid ice. In the frozen stage, the dielectric constant decreases continuously, and the *rms* height increases rapidly due to the completion of crystallization. In the thawing stage, the dielectric constant increases, and the *rms* height decreases owing to the melting of ice surface.

D. GA Results—Ice-Surface, Volume, and Ice-Bottom Scattering

Fig. 5(c) shows the backscattering components of the radar returns modeled by using the physical parameters of ice surface estimated by GA inversion. $\sigma^0_{surface}$, σ^0_{volume}, and σ^0_{bottom} are represented as black line with dots, triangles, and rectangles, respectively. Among them, $\sigma^0_{surface}$ was the strongest, giving a conclusion that the ice-surface scattering was the major component of the radar returns while σ^0_{bottom} is slightly higher than σ^0_{volume}. The change of $\sigma^0_{surface}$ generally follows the dielectric constant of the ice surface during the freezing and thawing stages, except for the frozen stage that follows the increase of *rms* height. σ^0_{bottom} and σ^0_{volume} is proportional to the transmissivity of ice body which is inversely proportional to the dielectric constant of the ice surface. Correlation length maintained rather constant and has little effect on the change of backscattering while *rms* height was a major contributing factor to the increase of $\sigma^0_{surface}$ [Fig. 5(b)]. This was probably because the sensitivity of *rms* height to $\sigma^0_{surface}$ modeling is higher than that of the correlation length in the IEM [36].

The interpretation of the change of backscattering during the freezing stage, frozen stage, and thawing stage can be as follows. During *the freezing stage*, $\sigma^0_{surface}$ weakened due to the decrease of dielectric constant of ice surface, whereas σ^0_{volume} and σ^0_{bottom} increased gradually owing to the higher transmissivity. In *the frozen stage* from 11:30 A.M. to 11:50 A.M., $\sigma^0_{surface}$, σ^0_{bottom} and σ^0_{volume} increased at the same time [Fig. 5(c)]. σ^0_{bottom} and σ^0_{volume} increased due to continuously decreasing dielectric constant of ice surface that lead to higher microwave transmissivity. The simultaneous increase of $\sigma^0_{surface}$ during the frozen stage was interpreted that the rapid increase of *rms* height by crystallization of the surface surpasses the decrease of dielectric constant. Consequently, $\sigma^0_{surface}$, σ^0_{bottom}, and σ^0_{volume} became strong simultaneously during the frozen stage. During *the thawing stage*, $\sigma^0_{surface}$ increased while σ^0_{bottom} and σ^0_{volume} decreased. The rapid increase of dielectric constant of melted surface water surpass the effect of lower *rms* height, resulting in the increase of $\sigma^0_{surface}$, while lower transmissivity reduced σ^0_{bottom} and σ^0_{volume}.

IV. Conclusion

This paper investigated the change of radar backscattering mechanism of lake ice during the freezing, frozen, and thawing stages of ice surface by using a ground-based scatterometer experiment and the inversion modeling of ice properties and scattering components by GA.

After spreading water over the ice surface, ice-surface scattering was strong whereas ice-bottom and volume scattering

was weak due to high dielectric constant of ice surface and low microwave transmissivity into the ice body. During the freezing stage of surface water, ice-surface scattering was reduced by the decrease of dielectric constant of ice surface. Ice-bottom and volume scattering, however, became strong by the increase of microwave transmissivity. When surface water was almost frozen, ice-surface scattering became strong due to large *rms* height by the crystallization of ice surface. Ice-bottom and volume scattering grew stronger due to large microwave transmissivity into the ice caused by low dielectric constant of the ice surface. Since air temperature rose above freezing, dielectric constant increased due to thawing of the ice surface. Then, ice-bottom and volume scattering became weak, whereas the ice-surface scattering was still strong. This study suggests that freezing/thawing of ice surface affects radar backscattering significantly and should be dealt with to clarify the microwave backscattering properties of ice, especially in phase transition of ice surface, and to better understand the diurnal and seasonal changes of ice observed from satellite SAR images.

REFERENCES

[1] M. A. Palecki and R. G. Barry, "Freeze-up and break-up of lakes as an index of temperature changes during the transition seasons: A case study for Finland," *J. Clim. Appl. Meteorol.*, vol. 25, no. 7, pp. 893–902, Jul. 1986.

[2] D. M. Livingstone, "Break-up dates of alpine lakes as proxy data for local and regional mean surface air temperatures," *Climatic Change*, vol. 37, no. 2, pp. 407–439, Oct. 1997.

[3] X. Fang and H. G. Stefan, "Potential climate warming effects on ice covers of small lakes in the contiguous U.S.," *Cold Reg. Sci. Technol.*, vol. 27, no. 2, pp. 119–140, Apr. 1998.

[4] G. Williams, K. L. Layman, and H. G. Stefan, "Dependence of lake ice covers on climatic, geographic and bathymetric variables," *Cold Reg. Sci. Technol.*, vol. 40, no. 3, pp. 145–164, Dec. 2004.

[5] R. N. Ghanbari, H. R. Bravo, J. J. Magnuson, and W. G. Hyzer, "Coherence between lake ice cover, local climate and teleconnections," *J. Hydrol.*, vol. 374, no. 3/4, pp. 282–293, Aug. 2009.

[6] S. E. Walsh, S. J. Vavrus, J. A. Foley, V. A. Fisher, R. H. Wynne, and J. D. Lenters, "Global patterns of lake ice phenology and climate: Model simulations and observation," *J. Geophys. Res.*, vol. 103, no. D22, pp. 28 825–28 837, Nov. 1998.

[7] J. J. Magnuson, D. M. Robertson, B. J. Benson, R. H. Wynne, D. M. Livingstone, T. Arai, R. A. Assel, R. G. Barry, V. Card, E. Kuusisto, N. G. Granin, T. D. Prowse, K. M. Stewart, and V. S. Vuglinski, "Historical trends in lake and river ice cover in the northern hemisphere," *Science*, vol. 289, no. 5485, pp. 1743–1746, Sep. 2000.

[8] S. J. Vavrus, R. H. Wynne, and J. A. Foley, "Measuring the sensitivity of southern Wisconsin lake ice to climate variations and lake depth using a numerical model," *Limnol. Oceanogr.*, vol. 41, no. 5, pp. 822–831, Jul. 1996.

[9] O. P. Jensen, B. J. Benson, J. J. Magnuson, V. M. Card, M. N. Futter, P. A. Soranno, and K. M. Stewart, "Spatial analysis of ice phenology trends across the Laurentian Great Lakes region during a recent warming period," *Limnol. Oceanogr.*, vol. 52, no. 5, pp. 2013–2026, Sep. 2007.

[10] S. V. Nghiem and G. A. Leshkevich, "Satellite SAR remote sensing of Great Lakes ice cover, Part I. Ice backscatter signature at C-band," *J. Great Lakes Res.*, vol. 33, no. 4, pp. 722–735, Dec. 2007.

[11] I. Gherboudj, M. Bernier, and R. Leconte, "A backscatter modeling for river ice: Analysis and numerical results," *IEEE Trans. Geosci. Remote Sens.*, vol. 48, no. 4, pp. 1788–1798, Apr. 2010.

[12] M. Nolan, G. Liston, P. Prokein, J. Brigham-Grette, V. L. Sharpton, and R. Huntzinger, "Analysis of lake ice dynamics and morphology on Lake El'gygytgyn, NE Siberia, using synthetic aperture radar (SAR) and Landsat," *J. Geophys. Res.*, vol. 107, p. 8162, Nov. 2002.

[13] C. R. Duguay, T. J. Pultz, P. M. Lafleur, and D. Drai, "RADARSAT backscatter characteristics of ice growing on shallow sub-Arctic lakes, Churchill, Manitoba, Canada," *Hydrol. Process.*, vol. 16, no. 8, pp. 1631–1644, Jun. 2002.

[14] M. O. Jeffries, K. Morris, W. F. Weeks, and H. Wakabayashi, "Structural and stratigraphic features and ERS 1 synthetic aperture radar backscatter characteristics of ice growing on shallow lakes in NW Alaska, winter 1991-1992," *J. Geophys. Res.*, vol. 99, no. C11, pp. 22 459–22 472, Nov. 1994.

[15] M. O. Jeffries, K. Morris, and G. E. Liston, "A method to determine lake depth and water availability on north slope of Alaska with spaceborne imaging radar and numerical ice growth modeling," *Arctic*, vol. 49, no. 4, pp. 367–374, Dec. 1996.

[16] N. Kozlenko and M. O. Jeffries, "Bathymetric mapping of shallow water in thaw lakes on the north slope of Alaska with spaceborne imaging radar," *Arctic*, vol. 53, no. 3, pp. 306–316, Sep. 2000.

[17] R. Leconte, S. Daly, Y. Gauthier, N. Yankielun, F. Bérubé, and M. Bernier, "A controlled experiment to retrieve freshwater ice characteristics from an FM-CW radar system," *Cold Reg. Sci. Technol.*, vol. 55, no. 2, pp. 212–220, Feb. 2009.

[18] I. Gherboudj, M. Bernier, F. Hicks, and R. Leconte, "Physical characterization of air inclusions in river ice," *Cold Reg. Sci. Technol.*, vol. 49, no. 3, pp. 179–194, Sep. 2007.

[19] M. P. Mäkynen, B. Cheng, M. H. Similä, T. Vihma, and M. T. Hallikainen, "Comparisons between SAR backscattering coefficient and results of a thermodynamic snow/ice model for the Baltic Sea land-fast sea ice," *IEEE Trans. Geosci. Remote Sens.*, vol. 45, no. 5, pp. 1131–1141, May 2007.

[20] W. Dierking, M. I. Pettersson, and J. Askne, "Multifrequency scatterometer measurements of Baltic Sea ice during EMAC-95," *Int. J. Remote Sens.*, vol. 20, no. 2, pp. 349–372, 1999.

[21] D. K. Perovich, J. Longacre, D. G. Barber, R. A. Maffione, G. F. Cota, C. D. Mobley, A. J. Gow, R. G. Onstott, T. C. Grenfell, W. S. Pegau, M. Landry, and C. S. Roesler, "Field observations of the electromagnetic properties of first-year sea ice," *IEEE Trans. Geosci. Remote Sens.*, vol. 36, no. 5, pp. 1705–1715, Sep. 1998.

[22] R. G. Onstott, "SAR and scatterometer signature of sea ice," in *Microwave Remote Sensing of Sea Ice*, F. Carsey, Ed. Washington, DC: Amer. Geophys. Union, 1992, ser. Geophysical Monograph 68, pp. 73–104.

[23] T. Geldsetzer, J. B. Mead, J. J. Yackel, R. K. Scharien, and S. E. L. Howell, "Surface-based polarimetric C-band scatterometer for field measurements of sea ice," *IEEE Trans. Geosci. Remote Sens.*, vol. 45, no. 11, pp. 3405–3416, Nov. 2007.

[24] D. Isleifson, A. Langlois, D. G. Barber, and L. Shafai, "C-band scatterometer measurements of multiyear sea ice before fall freeze-up in the Canadian Arctic," *IEEE Trans. Geosci. Remote Sens.*, vol. 47, no. 6, pp. 1651–1661, Jun. 2009.

[25] K. C. Partington, J. D. Flach, D. Barber, D. Isleifson, P. J. Meadows, and P. Verlaan, "Dual-polarization C-band radar observations of sea ice in the Amundsen Gulf," *IEEE Trans. Geosci. Remote Sens.*, vol. 48, no. 6, pp. 2685–2691, Jun. 2010.

[26] C. E. Livingstone and M. R. Drinkwater, "Springtime C-band SAR backscatter signatures of Labrador Sea marginal ice: Measurements versus modeling predictions," *IEEE Trans. Geosci. Remote Sens.*, vol. 29, no. 1, pp. 29–41, Jan. 1991.

[27] S. Tjuatja, A. K. Fung, and J. Bredow, "A scattering model for snow-covered sea ice," *IEEE Trans. Geosci. Remote Sens.*, vol. 30, no. 4, pp. 804–810, Jul. 1992.

[28] A. Carlström and L. M. H. Ulander, "Validation of backscatter models for level and deformed sea-ice in ERS-1 SAR images," *Int. J. Remote Sens.*, vol. 16, no. 17, pp. 3245–3266, 1995.

[29] A. Carlström, "A microwave backscattering model for deformed first-year sea ice and comparisons with SAR data," *IEEE Trans. Geosci. Remote Sens.*, vol. 35, no. 2, pp. 378–391, Mar. 1997.

[30] P. S. Ray, "Broadband complex refractive indices of ice and water," *Appl. Opt.*, vol. 11, no. 8, pp. 1836–1844, Aug. 1972.

[31] M. N. O. Sadiku, "Refractive index of snow at microwave frequencies," *Appl. Opt.*, vol. 24, no. 4, pp. 572–575, Feb. 1985.

[32] A. K. Fung, *Microwave Scattering and Emission Models and Their Applications*. Boston, MA: Artech House, 1994.

[33] R. Leconte and P. D. Klassen, "Lake and river ice investigations in northern Manitoba using airborne SAR imagery," *Arctic*, vol. 44, no. 5, pp. 153–163, 1991.

[34] P. C. Mullen and S. G. Warren, "Theory of the optical properties of lake ice," *J. Geophys. Res.*, vol. 93, no. D7, pp. 8403–8414, Jul. 1988.

[35] D. E. Goldberg, *Genetic Algorithm in Search, Optimization and Machine Learning*. Reading, MA: Addison-Wesley, 1989.

[36] M. M. Rahman, M. S. Moran, D. P. Thoma, R. Bryant, E. E. Sano, C. D. H. Collins, S. Skirvin, C. Kershner, and B. J. Orr, "A derivation of roughness correlation length for parameterizing radar backscatter models," *Int. J. Remote Sens.*, vol. 28, no. 18, pp. 3995–4012, Sep. 2007.

Hyangsun Han (S'06) was born in Chuncheon, Korea, in August 1982. He received the B.S. and M.S. degrees in geophysics from Kangwon National University, Chuncheon, in 2006 and 2008, respectively. He is studying for the Ph.D. degree.

His research interests include microwave remote sensing of polar glaciers, sea ice, lake ice, ocean, and land surfaces. He is also interested in various applications of remotely sensed data using synthetic aperture radar and interferometry, and geophysical modeling and inversion problems.

Mr. Han received Student Paper Awards at the Korea Remote Sensing Symposia in 2006 and 2007.

Hoonyol Lee (S'99–M'01–SM'11) was born in Kwangju, Korea, in 1969. He received the B.S. degree in geology in 1995 and the M.S. degree in geophysics in 1997, both from Seoul National University, Seoul, Korea, and the Ph.D. degree of radar remote sensing from Imperial College London, University of London, U.K., in 2001.

From 2001 to 2003, he was a Postdoctoral Research Associate with Imperial College London, U.K. From 2003 to 2004, he was a Senior Researcher with the Korea Institute of Geoscience and Mineral Resources, Daejeon, Korea. Since 2004, he has been with the Department of Geophysics, Kangwon National University, Korea, where he is currently an Associate Professor. From August 2008 to July 2009, he was a Visiting Scholar with the Department of Geological Sciences, University of Oregon. His research interests include synthetic aperture radar (SAR), interferometry, and polarimetry. He developed an educational synthetic aperture radar (eSAR) processor, a SAR ocean processor, polarimetric scatterometer systems, and ground-based SAR systems.

Prof. Lee was supported by the Korean Ministry of Education Scholarship, the Overseas Research Student Award from the Committee of Vice-Chancellor and Principals, U.K., and the Chevening Scholarship from British Embassy in Korea, for his Ph.D. study. He was awarded the Interactive Session Prize Paper Award at the 1999 IEEE International Geoscience and Remote Sensing Symposium, Hamburg, Germany. In 2008, he received the Best Paper Award of *Korean Journal of Remote Sensing*. He is a Senior Member of IEEE Geoscience and Remote Sensing Society and a member of American Geophysical Union. From 2011, he serves as the Editor of the *Korean Journal of Remote Sensing*.